Design of a grating-based thin-film filter for broadband spectropolarimetry

Donghyun Kim and Kieron Burke

We propose a simple procedure for designing an integrated single-chip grating-based thin-film filter. A simulation from a rigorous coupled-wave analysis shows that structural adjustment based on the effective medium theory can achieve the desired integration without notable performance degradation. Our spectropolarimetric filter design maintains spectral filter characteristics, while its extinction ratio is significantly enhanced over the passband. The integrated spectropolarimetric filter can be a basis for building multispectral multipolarimetric filters for spectropolarimetry in remote-sensing applications. © 2003 Optical Society of America

OCIS codes: 120.2440, 130.3120, 230.4170.

1. Introduction

The wire-grid grating provides excellent discrimination between polarization components and is relatively easy to design and fabricate. Many researchers thus are drawn to grating-based polarization-sensitive devices such as polarization beam splitters[1,2] and polarimetric photodiodes,[3,4] and wire-grid polarization filters are even commercially available.

Although the wire-grid grating is widely used in polarization-sensing applications, it is yet to make a notable contribution to the implementation of multispectral polarimetric filter (MSPF) systems for spectropolarimetry. MSPF systems typically employ less than 10 wavebands for spectral information and are based on the complementarity of spectral and polarimetric measurements to increase the probability of finding a target object against a given natural background. Although recently they have been a subject of intensive research, previously explored multispectral and/or polarization systems were primarily built with discrete components, including the use of separate optical channels in parallel to detect multispectral and polarization signatures,[5–7] the use of acousto-optic tunable filters[8,9] or fast-spinning spectral filters that can also measure polarization states,[10,11] and measurement of the Mueller matrix of a sample with Fourier-transform-infrared spectroscopy followed by polarization analysis.[12,13] Numerous polarimetric measurement systems operating in a single spectral band have also been investigated. Some of these are based on wire-grid polarizers,[14,15] diffraction gratings,[16] Brewster plates,[17] or special prisms.[18,19] Not only are most of these discrete systems bulky, but their performance is also extremely sensitive to alignment among optical components. We can attain the highest precision by integrating a MSPF to have spectral and polarimetric data perfectly registered without involving any mechanically moving part in the system. Integration also saves space in space-limited applications such as missiles and satellites so that the saved space can be reassigned for extra capability. Despite these apparent advantages from integrating polarizers with spectral filters in a compact single package, few researchers have attempted to integrate largely because of the relative difficulty associated with building one filter on top of the other, compared with the wide availability of off-the-shelf discrete components.

The wire-grid grating is planar in structure, which makes vertical integration onto a spectral filter convenient. However, a wire-grid polarizer, if directly integrated onto a spectral filter, generally interferes with the spectral characteristics of the spectral filter or results in side effects such as guided-mode resonance.[20] To prevent this, integration was previously presumed to require an isolation layer between two filters, the optimization of which may be difficult.

In this paper we explore a procedure for designing a wire-grid polarizer directly integrated onto a thin-film spectral filter on a common substrate, which exhibits the desired spectral and polarimetric performance without any isolation layer. A broadband spectrum for multispectral polarimetry is obtained as a result of integration, taking advantage of the characteristics of the thin-film bandpass filter (BPF). In this research we describe the theoretical evolution of our previous work in which our design approach was experimentally verified for thin-film filters while a wire-grid polarizer was mechanically sandwiched to a spectral filter to form an imaging multispectral polarimetric system.[21]

2. Filter Design

Polarization-sensitive devices are typically designed by using an effective medium theory (EMT), according to which a periodic structure may be replaced with an anisotropic homogeneous medium if only the zeroth diffraction order propagates and higher diffraction orders are evanescent.[22] The EMT provides a simple second-order expression in closed form to give the effective index of a grating for $\Lambda \ll \lambda$, with Λ and λ being, respectively, the grating period and the free-space wavelength of incident light. Namely,

$$\varepsilon_{\mathrm{eff,TE}}^{(2)} = \varepsilon_{0,\mathrm{TE}} + \frac{\pi^2}{3} f^2 (1-f)^2 (\varepsilon_A - \varepsilon_B)^2 \left(\frac{\Lambda}{\lambda}\right)^2,$$

$$\varepsilon_{\mathrm{eff,TM}}^{(2)} = \varepsilon_{0,\mathrm{TM}} + \frac{\pi^2}{3} f^2 (1-f)^2 \left(\frac{1}{\varepsilon_A} - \frac{1}{\varepsilon_B}\right)^2$$
$$\times \varepsilon_{0,\mathrm{TM}}^3 \varepsilon_{0,\mathrm{TE}} \left(\frac{\Lambda}{\lambda}\right)^2, \quad (1)$$

where f is the grating fill factor and ε_A and ε_B are the relative permittivities of the grating materials. The zero-order permittivity ε_0 in Eq. (1) is given by

$$\varepsilon_{0,\mathrm{TE}} = f\varepsilon_A + (1-f)\varepsilon_B, \quad \varepsilon_{0,\mathrm{TM}} = \frac{\varepsilon_A \varepsilon_B}{f\varepsilon_B + (1-f)\varepsilon_A} \quad (2)$$

for TE- and TM-polarization components. Unfortunately, the metallic gratings used to realize a high extinction ratio (ER), defined as the intensity ratio between the TM and TE polarization components, have a large negative permittivity. The second-order polynomial expressions in Eq. (1) therefore do not result in a well-converged effective index, and closed-form solutions from the EMT do not exist for metallic gratings. In this paper the effective index is found by simulating the filter structure with a rigorous coupled-wave analysis (RCWA) and then fitting the result with a transmittance curve. Based on a full vector implementation, our RCWA routine reduces Maxwell equations to a simple algebraic eigenvalue problem.[23,24] We focus on the TM-polarization component, since TE polarization is mostly reflected by the wire-grid polarizer and becomes negligible within a thin-film filter when the

wire-grid polarizer and the thin-film filter are integrated.

Suppose a thin-film filter that consists of m layers with n_i and d_i as a refractive index and a thickness of the ith layer, respectively. Our approach to implementing an integrated spectropolarimetric filter (SPF) is first to separately design a multispectral thin-film filter and a wire-grid grating for a target spectral range. The wire-grid grating needs to be sufficiently thick so that the evanescent modes created at the top and bottom grating interfaces do not tunnel through. The top-layer thickness of the spectral filter that interfaces the wire-grid polarization filter is then adjusted based on the effective index of the wire-grid grating, so that when the spectral filter and the wire-grid grating are integrated on a single substrate, they operate as a SPF. Last, the thin-film thickness of the designed SPF can be changed to form a pixelated MSPF system.

A. Spectral Filter Design

Our design aimed at a SPF for the 3–5-μm mid-wave infrared (MWIR) range. With simulated annealing, three four-layer thin-film BPFs were designed for center wavelengths at 3.5, 4.0, and 4.5 μm and a spectral bandwidth of 0.5 μm.[21] Three wavebands were selected for multispectral polarimetry by analogy with three primary colors. In this paper we consider the BPF centered at 4.0 μm, which was optimized as Ge(2500 Å)/SiO(11000 Å)/Ge(2500 Å)/ SiO(4500 Å), using Ge and SiO as high- and low-index materials on a GaAs substrate. The major design requirements for the spectral filter were a minimal number of layers to ensure reproducible and reliable experiments and yet an easy-to-shift center wavelength for realizing multispectral bands. With this design the thickness of the second SiO layer between the Ge films can be used to shift the center wavelength. Since this interference filter was optimized only for the 3–5-μm range, it is necessary to cascade the interference filter with long-pass and short-pass absorption filters to reject light outside this range. Its operation was experimentally confirmed after the filter was constructed on silicon and GaAs substrates.[21] Note that the refractive index of SiO changes slightly, depending on the deposition rate and other parameters.[25] With our calculation it was 1.835 at $\lambda = 4.0$ μm with the Herzberger model.[26] For reference the refractive index of Ge and GaAs used in the design is 4.0 and 3.3, respectively, at $\lambda = 4.0$ μm.

B. Polarization Filter Design

The wire-grid polarization filter is assumed to be of 2000-Å-thick Al with a 0.4-μm period and a 50% fill factor. Aluminum provides an excellent polarization contrast when used to fabricate a wire-grid polarizer and offers a variety of processing possibilities. The minimum thickness of a wire-grid grating is determined by the skin depth of the grating material, which is typically of the order of 200 Å at optical frequencies for Al. In our design the Al thickness of
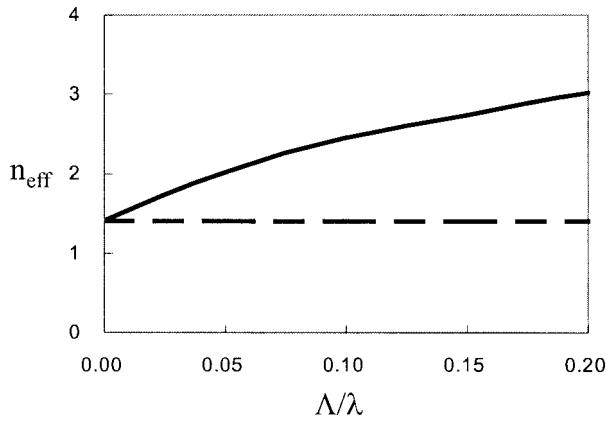
Fig. 1. Effective index n_{eff} of the wire-grid grating polarization filter for incident light with a wavelength of $\lambda = 4.0$ μm. The filter is made of aluminum, 2000 Å thick: solid curve, effective index obtained by fitting the RCWA results with transmittance calculations, assuming negligible absorption; dashed line, zeroth-order effective index from the effective medium theory of Eq. (2).

Fig. 2. Designed SPF structure with the effective index calculated in Fig. 1.

the wire grids was selected to be 10 times the skin depth. A higher ER can be generally achieved with a thicker grating because the TE polarization is further absorbed by metallic wire grids while the TM component remains fairly constant. The maximum thickness may be limited by the aspect ratio permitted by the lift-off and dry-etching process to fabricate the grating. The effect of the grating thickness on the spectral characteristics is discussed in detail in Section 3.

Figure 1 shows the effective refractive index of this grating with respect to the ratio of the grating period to the free-space wavelength of the incident light at 4.0 μm. The solid curve represents the effective index n_{eff} of the grating layer that most closely fits the RCWA results when a homogeneous layer with n_{eff} replaces the grating layer. The long-wavelength limit $n_{eff}^{(0)} = (\varepsilon_0)^{1/2}$ from Eq. (2) is also shown as a dashed line for comparison. The fit assumes negligible absorption in the effective medium, which is generally valid for TM polarization. The second-order effective index $n_{eff}^{(2)} = [\varepsilon_{eff}^{(2)}]^{1/2}$ from Eq. (1) is not shown in Fig. 1, since it becomes imaginary owing to the large negative permittivity of the metal (Al in this case).

For our design the period-to-wavelength ratio was selected to be $\Lambda/\lambda = 0.10$ at which the effective index of the grating $n_{eff} = 2.45$. Only the zeroth diffraction order is present in the system, since $\lambda > n_s\Lambda$ with this ratio. If $\lambda < n_s\Lambda$ with n_s for the substrate refractive index, the transmittance is reduced by higher-order diffraction, degrading the ER. Note that the refractive index of GaAs is used as n_s for a stand-alone wire-grid polarizer, and it is that of Ge for a SPF in which the grating is on top of a Ge film. On the other hand, an extremely small Λ/λ, while it may make the EMT polynomial equations hold even for metallic grating, is not physically useful since such small wire grids are difficult to produce.
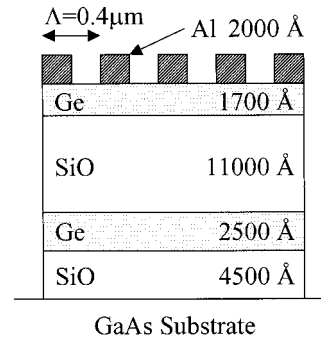
C. Integration

The top-layer thickness of the designed spectral filter can be adjusted so that the optical path length is maintained, i.e., $n_m d_m = n_{eff}d_{grating} + n_m d_m'$, where d_m' is the adjusted top-layer thickness. Since the equivalency of the optical path length holds for only one wavelength and a SPF is designed for a broad waveband, d_m' needs to be further optimized from the value determined by the equivalency of the optical path length, which can be done with a RCWA. Since $n_{eff} \neq n_m$ in general, multiple reflection occurs at the interface between the spectral and polarization filters, which leads to degradation in the spectral performance.

Although different approaches are possible to designing a single-chip SPF, such as inserting a wire-grid grating between or on the bottom of thin-film layers and changing a grating period instead of the top-layer thickness of the spectral filter, these alternative approaches are deemed impractical to implement physically. The generic procedure described in this paper is relatively simple and can be applied to any spectral BPF structure.

3. Results

The final design for $\Lambda/\lambda = 0.10$ is shown in Fig. 2, where the top-layer thickness d_m' of the spectral filter is determined to be 1700 Å. The spectral and polarization characteristics of the designed SPF, calculated with the RCWA, are shown in Figs. 3 and 4, respectively. In Fig. 3 the spectral characteristics for the TM polarization of the SPF in Fig. 2, compared with the original spectral filter without a grating, shows that the spectral performance is not significantly affected by the presence of the wire-grid polarization filter. With our design the multiple reflection at the interface between the grating and the top layer of the spectral filter causes the half-width to be broadened from 0.3 to 0.4 μm and the spectral shape to become slightly asymmetric. The peak transmittance is also reduced by 6%.

Figure 4 shows the polarization contrast of the designed SPF compared with the wire-grid polarization filter on a GaAs substrate. The Al grating is 2000 Å thick with a 50% fill factor and 0.4-μm period in both cases. The polarization response of the SPF shows
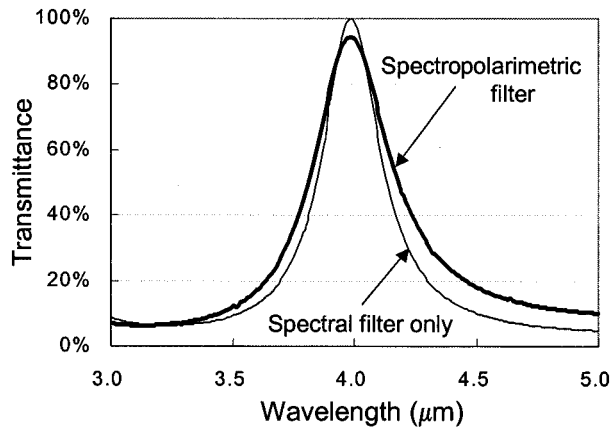
Fig. 3. Transmittance of the designed SPF compared with that of the original spectral filter design without a grating. The transmittance was calculated by the RCWA.

strong spectral dependence and considerable enhancement of the ER over the passband, while the ER is relatively flat without the spectral filter. The TE transmission is mostly absorbed and reflected by metallic wire grids so that it is affected little by the spectral filter. Thus TE transmission has few BPF characteristics over the passband, as is clear in Fig. 5(a). On the contrary, since the TM transmission is transmitted through the metallic grating, the TM transmittance maintains the spectral characteristics of the underlying spectral filter, as shown in Fig. 5(b). The improvement in the ER over the passband is attributed to the reduced TE transmittance and increased TM transmittance after integration as a result of the interaction between the grating underlying the multilayer thin films. For the TM mode, the effective index of which is available, a ballpark estimation for the increased TM transmittance can be made by calculating a first-order reflectance at $\lambda = 4.0$ μm at the interface between the grating and an underlying layer. The reflectance at the interface, $R_{TM} = (n_{grating,TM} - n)^2/(n_{grating,TM} + n)^2$ with n as the refractive index of the underlying layer, is
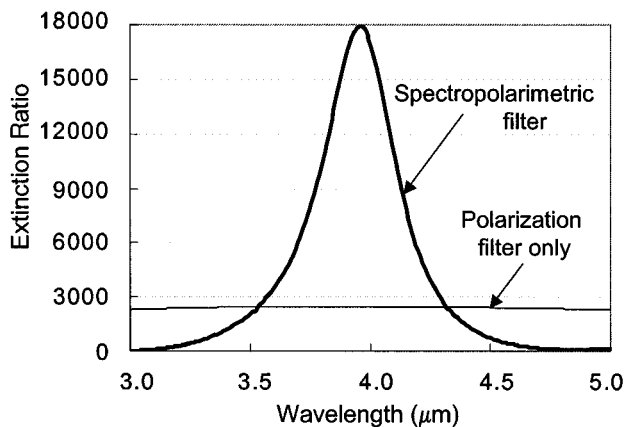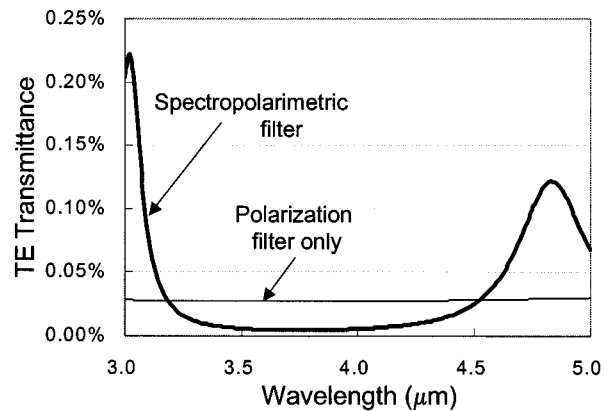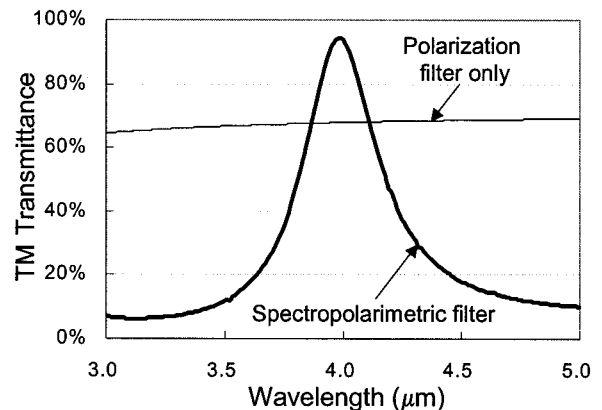

Fig. 4. Extinction ratio of the designed SPF compared with that of the wire-grid polarization filter with 2000-Å-thick Al and Λ = 0.4 μm.
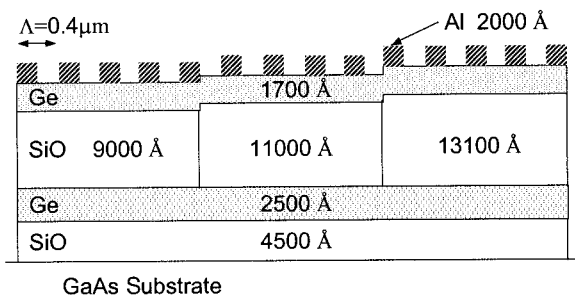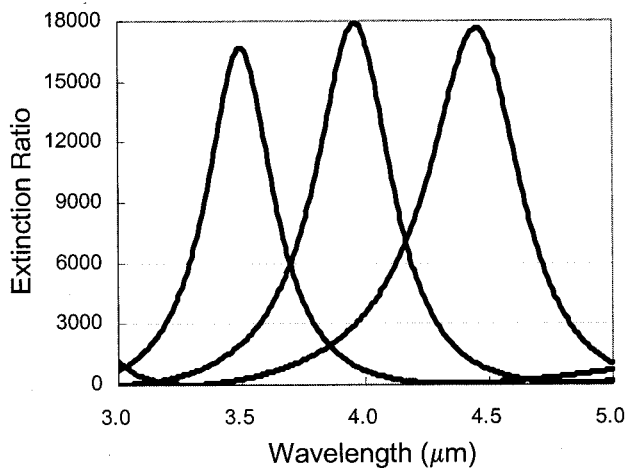

(a)

(b)

Fig. 5. Transmittance of (a) TE- and (b) TM-polarization components of the designed SPF compared with that of the wire-grid grating polarization filter with 2000-Å-thick aluminum and Λ = 0.4 μm.

17% and 6% for a stand-alone grating ($n = n_{air}$) and a SPF ($n = n_{Ge}$), respectively. This is roughly in agreement with Fig. 5(b).

Note that the results of the BPF characteristics for TM transmission were reported for subwavelength wire-grid polarizers at a visible light wavelength in Refs. 2, 27, and 28. A stand-alone polarizer not coupled to a spectral filter, however, typically results in narrow passbands, where the optimal design over a peak wavelength and bandwidth is not straightforward. It is possible to obtain broadband BPF characteristics desired for multispectral polarimetry by combining a wire-grid polarizer with a spectral filter because, when a wire-grid polarizer is integrated, the design parameters of the wire-grid polarizer and the spectral filter can be modified to shift the spectral characteristics of the two filters so that a relatively flat spectral response of the wire-grid polarizer (See Fig. 5) is coupled to the broadband BPF characteristics of the spectral filter. Therefore an integrated SPF preserves the spectral characteristic of the spec-

$\Lambda = 0.4\mu m$

Al 2000 Å

Ge 1700 Å

SiO 9000 Å   11000 Å   13100 Å

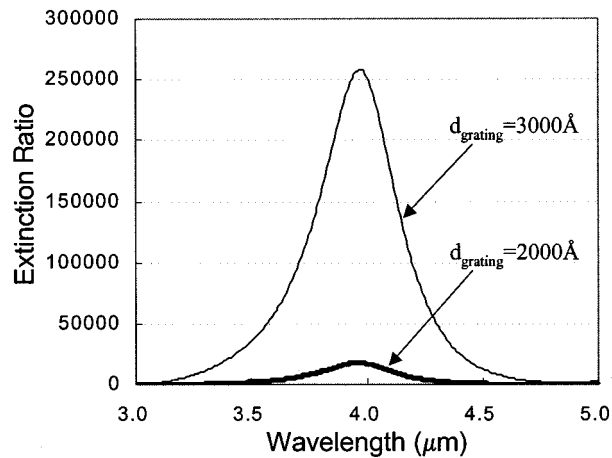Ge 2500 Å

SiO 4500 Å

GaAs Substrate

(a)

(b)

Fig. 6. Single-chip multispectral polarimetric filter designed by varying the thickness of middle SiO layer based on the SPF design in Fig. 2. (a) Structural schematic showing the peak wavelength of extinction ratio designed to be at 3.5, 4.0, and 4.5 μm when a SiO layer thickness of 9000, 11000, and 13100 Å, respectively, is chosen. (b) Corresponding spectrum of the extinction ratio.

$d_{grating}$=3000Å

$d_{grating}$=2000Å

(a)

$d_{grating}$=2000Å

$d_{grating}$=3000Å

(b)

Fig. 7. Effect of grating thickness on the (a) extinction ratio and (b) transmittance of the TM-polarization component of the SPF. Bold and regular solid curves, filter performance when grating thicknesses of 2000 and 3000 Å, respectively, with other structural parameters unchanged.
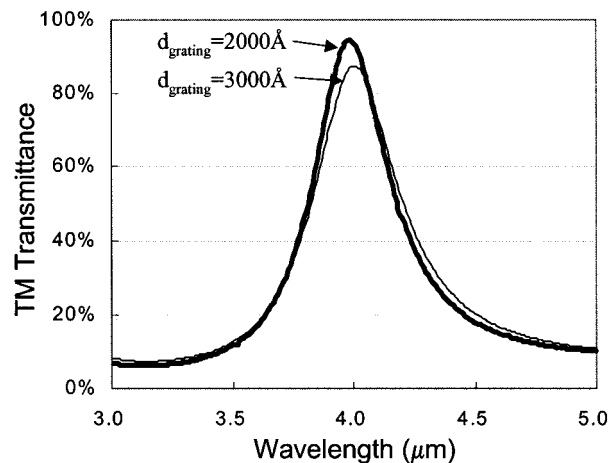
tral filter (See Fig. 3), while it achieves a high ER characteristic of the wire-grid polarizer.

Since its spectrum is easily shifted in wavelength when the thin-film thickness is changed, a multispectral and multipolarimetric filter can be formed based on the designed structure of Fig. 2 by pixelating the SPFs with different spectral and polarimetric properties. Figure 6 presents a single-chip trispectral polarimetric filter with peak wavelengths of 3.5, 4.0, and 4.5 μm. This structure is obtained by varying the middle SiO layer thickness to be 9000, 11000, and 13100 Å, respectively, as shown in Fig. 6(a). The spectra of the ER in Fig. 6(b) exhibit the bandpass characteristics for multiple wavebands. The relative nonuniformity in the peak ER among the three wavebands ($\equiv |ER_{max} - ER_{min}|/ER_{min}$) is approximately 6.4%. However, the peak transmittance of the TM polarization is fairly uniform with a relative nonuniformity of less than 1%.

The effect of the grating thickness is also investigated for a SPF. Note that it is relatively difficult to

check the effect on a wire-grid polarizer itself because of the extremely flat transmittance, as shown in Fig. 5, owing to the small period of the grating. Figure 7(a) shows that the grating thickness has little influence on the peak location of the SPF spectrum, while a thicker wire-grid grating increases the ER significantly. The ER is increased 14.5 times as the grating thickens from 2000 to 3000 Å. Figure 7(b) shows that the spectral shape and half-width of the SPF remain almost unchanged, except that the transmittance is reduced by 7%. These results indicate that the grating thickness does not noticeably affect the n_{eff} of the grating and spectral characteristics of the designed SPF, as can be qualitatively deduced from Eqs. (1) and (2), which do not depend on thickness. The major effect of the grating thickness is on the TE polarization. With a thicker grating, the TE component is more absorbed, whereas the TM polarization stays constant in intensity, resulting in an enhanced ER. The grating thick-

ness can therefore be used effectively to obtain the desired polarization contrast in a SPF.

For the actual fabrication of pixelated multispectral multipolarimetric filters, aluminum wires can be patterned from electron-beam or UV lithography. Commercial lithographic systems typically and routinely produce features much smaller than 0.2 μm with large depths of focus. On the other hand, the implementation of multipolarimetric pixels of different wire orientations may be subject to the variations in polarization contrast owing to the line-edge roughness that occurs when wires are made in all directions simultaneously in an integrated fashion. The extent of the variation should depend on specific fabrication processes.

4. Concluding Remarks

We have proposed a simple design for integrating spectral and polarization filters on a single substrate. RCWA simulation shows that the desired integration can be achieved without significant performance degradation, if individually designed thin-film spectral and wire-grid polarization filters are structurally adjusted based on the EMT. Thus the designed SPF maintains spectral filter characteristics, while its ER is improved considerably over the passband. The SPF is expected to be useful for building multispectral multipolarimetric filters for remote-sensing applications.

Even though our initial effort is focused on optical coupling of the designed SPF with a detector, the direct integration of the SPF onto a detector is also of great interest as a natural evolution of this research. Previous attempts to integrate a wire-grid polarizer with a detector confirm that polarization selection over the passband can be achieved by direct integration with additional fabrication steps to deposit thin films on a photodetector.[3,4] In the case of optimizing thin-film layers on a photodetector, only boundary conditions may change from the air to a specific substrate.

References

1. R. C. Tyan, A. A. Salvekar, H. P. Chou, C. C. Cheng, A. Scherer, P. C. Sun, F. Xu, and Y. Fainman, "Design, fabrication, and characterization of a form-birefringent multilayer polarizing beam splitter," J. Opt. Soc. Am. A **14,** 1627–1636 (1997).

2. P. Lalanne, J. Hazart, P. Chavel, E. Cambril, and H. Launois, "A transmission polarizing beam splitter grating," J. Opt. A: Pure Appl. Opt. **1,** 215–219 (1999).

3. T. Doumuki and H. Tamada, "An aluminum-wire grid polarizer fabricated on a gallium-arsenide photodiode," Appl. Phys. Lett. **71,** 686–688 (1997).

4. E. Chen and S. Y. Chou, "Polarimetry of thin metal transmission gratings in the resonance region and its impact on the response of metal–semiconductor–metal photodetectors," Appl. Phys. Lett. **70,** 2673–2675 (1997).

5. W. G. Egan, "Proposed design of an imaging spectropolarimeter/photopolarimeter for remote sensing of earth resources," Opt. Eng. **25,** 1155–1159 (1986).

6. L. D. Travis, "Remote sensing of aerosols with the Earth Observing Scanning Polarimeter," in *Polarization and Remote Sensing*, W. G. Egan, ed., Proc. SPIE **1747,** 154–164 (1992).

7. B. H. Miles, E. R. Cespedes, and R. A. Goodson, "Polarization-based active/passive scanning system for minefield detection," in *Polarization and Remote Sensing*, W. G. Egan, ed., Proc. SPIE **1747,** 239–252 (1992).

8. D. A. Glenar, J. J. Hillman, B. Saif, and J. Bergstrahl, "Polaris II: an acousto-optic imaging spectropolarimeter for ground-based astronomy," in *Polarization and Remote Sensing*, W. G. Egan, ed., Proc. SPIE **1747,** 92–103 (1992).

9. H. Takami, H. Shiba, S. Sato, T. Yamashita, and Y. Kobayashi, "A near-infrared prism spectrophotopolarimeter," Publ. Astron. Soc. Pac. **104,** 949–954 (1992).

10. P. Y. Deschamps, M. Herman, A. Podaire, and A. Ratier, "The POLDER instrument: mission objectives," in *Polarization and Remote Sensing*, W. G. Egan, ed., Proc. SPIE **1747,** 72–91 (1992).

11. K. P. Bishop, H. D. McIntire, M. P. Fetrow, and L. McMackin, "Multispectral polarimeter imaging in the visible to near IR," in *Targets and Backgrounds: Characterization and Representation V*, W. R. Watkins, D. Clement, and W. R. Reynolds, eds., Proc. SPIE **3699,** 49–57 (1999).

12. D. B. Chenault and R. A. Chipman, "Infrared spectropolarimetry," in *Polarization Considerations for Optical Systems II*, R. A. Chipman, ed., Proc. SPIE **1166,** 254–266 (1989).

13. J. L. Pezzaniti and R. A. Chipman, "Mueller matrix imaging polarimeter," Opt. Eng. **34,** 1558–1568 (1995).

14. C. S. L. Chun, D. L. Fleming, W. A. Harvey, E. J. Torok, and F. A. Sadjadi, "Synthetic vision using polarization-sensitive, thermal imaging," in *Enhanced and Synthetic Vision*, J. G. Verly, ed., Proc. SPIE **2736,** 9–20 (1996).

15. G. P. Nordin, J. T. Meier, P. C. Deguzman, and M. W. Jones, "Micropolarizer array for infrared imaging polarimetry," J. Opt. Soc. Am. A **16,** 1168–1174 (1999).

16. R. M. A. Azzam and K. A. Giardina, "Photopolarimeter based on planar grating diffraction," J. Opt. Soc. Am. A **10,** 1190–1196 (1993).

17. J. R. Maxwell and T. J. Rogne, "Advances in polarized infrared imaging, Part 1," in *Spectral Reflections IRIA Newsletter* **97-01** (1997).

18. W. A. Shurcliff, *Polarized Light: Production and Use* (Harvard University, Cambridge, Mass., 1962).

19. E. Oliva, "Wedged double Wollaston, a device for single-shot polarimetric measurements," Astron. Astrophys. Suppl. Ser. **123,** 589–592 (1997).

20. R. Magnusson and S. S. Wang, "Transmission bandpass guided-mode resonance filters," Appl. Opt. **34,** 8106–8109 (1995).

21. D. Kim, C. Warde, K. Vaccaro, and C. Woods, "Imaging multispectral polarimetric sensor: single pixel design, fabrication, and characterization," Appl. Opt. **42,** 3756–3764 (2003).

22. S. M. Rytov, "Electromagnetic properties of a finely stratified medium," Sov. Phys. JETP **2,** 466–475 (1956).

23. M. G. Moharam and T. K. Gaylord, "Diffraction analysis of dielectric surface-relief gratings," J. Opt. Soc. Am. **72,** 1385–1392 (1982).

24. M. G. Moharam and T. K. Gaylord, "Rigorous coupled-wave analysis of metallic surface-relief gratings," J. Opt. Soc. Am. A **3,** 1780–1787 (1986).

25. W. A. Pliskin and H. S. Lehman, "Structural evaluation of silicon oxide films," J. Electrochem. Soc. **112,** 1013–1019 (1965).

26. M. Herzberger, "Color correction in optical systems and a new dispersion formula," Opt. Acta **6,** 197–215 (1959).

27. S. Astilean, P. Lalanne, and M. Palamaru, "Light transmission through metallic channels much smaller than the wavelength," Opt. Commun. **175,** 265–273 (2000).

28. Z. Yu, P. Deshpande, W. Wu, J. Wang, and S. Y. Chou, "Reflective polarizer based on a stacked double-layer subwavelength metal grating structure fabricated using nanoimprint lithography," Appl. Phys. Lett. **77,** 927–929 (2000).